State of art and next challenges in instrumentation for quality control in hadrontherapy centres

S. Karkar, N. Pauna, E. Testa

Ref. LPC: PCCF RI 0801 Ref.INPL: LYCEN 2008-02 Ref.CPPM: CPPM-P-2008-01

State of art and next challenges in instrumentation for quality control in hadrontherapy centres

S. Karkar[1], *N. Pauna*[2], *E. Testa*[3]
INNOTEP collaboration

[1]Centre de Physique des Particules de Marseille,
CPPM, Aix-Marseille Université, CNRS/IN2P3, Marseille, France
[2]Laboratoire de Physique Corpusculaire,
LPC Clermont, Université Blaise Pascal, CNRS/IN2P3, Aubière, France
[3]Institut de Physique Nucléaire de Lyon,
IPNL, Université de Lyon, CNRS/IN2P3, Villeurbanne, France

Abstract

In this document we aim at summarising the different points so far addressed and those that are still to be resolved in instrumentation for quality control in hadrontherapy centres. This includes on line in beam PET for dose deposition monitoring, beam hodoscope and prompt gamma monitoring.

Contents

Chapter 1

Introduction

The in-beam positron emission tomography (PET) is currently the only feasible non-invasive method for in-situ monitoring of tumour treatments with ion beams. It is able of assessing parameters relevant for quality assurance, i.e. the particle range in tissue, the position of the irradiated volume and the local deviations between planned and applied distributions.
Worldwide, there are two approaches for estimating the dose delivery in hadron-therapy centers. The first one, applied at the Heavy Ion Medical Accelerator in Chiba (Japan), is an off-beam PET: the β^+ emitter distribution induced in the patient by the irradiation is measured with a commercial PET outside of the irradiation room. The advantage of such approach is that it does not require particular developments but the moving of the patient from the treatment site to the PET scanner introduces large uncertainties. The second technique is an in-beam PET. It was used for the first time for quality assurance at GSI hadron-therapy center since 1997 : the acquisition is performed during the irradiation and some minutes after which allows the detection of both short-lived and long-lived isotopes and avoids to move the patient. Moreover we can imagine that such in-line PET could be improved to become an on-line PET in conditions that number of LOR detected (Lines of Responses) is large enough and time of reconstruction is short enough to provide typically an image every tens of seconds.
The objectives pursued with the present work are to outline present limitations and future challenges of in-beam PET instrumentation. Present limitations are those already existing at the in-beam PET from GSI: the detector and data acquisition technology is based on the solutions available at the time of its installation. Besides limitations arising from limited angle tomography, in-beam PET images are also affected by low statistics data. Data taking during particle beam extraction is presently vetoed due to the presence of a high noise background which overlaps the coincidence signal.
Since then, not only the state-of-the-art technology has out performed the efficiency of the tomography once installed at GSI facility, as well as the special requirements of in-beam PET have been better understood. Future challenges are those expected to arise at in-beam PET installed onto heavy ion tumour treatment facilities under planning or construction (e.g. HIT, Heidelberg Ion Beam Therapy Centre, Germany). As an example, a magnetic field resistant detector is necessary if the in-beam PET scanner is operated close to the last

bending magnet, as is the case at the HIT facility with a beam gantry (e.g. isocentric, rotating beam deliveries).
The aim of Part I is to present the prerequisites for a in-beam PET system as well as recent studies to optimise the detector geometry and its performances (by testing modern gamma ray detectors) as well as data processing methods (including adapted reconstruction methods for PET data). It mainly describes several mathematical and technological innovative solutions proposed, constructed and verified, either by simulation or experimentally, in the PhD thesis work of P. Crespo (Darmstadt, 2005).
In Part II, in-beam and on-line PET challenges are identified. Performances of new fast scintillators and photodetectors are presented in correlation with expected tasks for an optimal delivered dose monitoring. The need of additional simulations for estimating the feasibility of a real time PET camera is obvious. This part also includes a discussion about the possibility of using gamma prompt radiation as a monitor of the dose inside patient under certain conditions.

Part I

State of the art: PET in hadrontherapy centres

Chapter 2

Geometry

The first attempts in operating an in-beam positron tomograph at the Lawrence Berkeley National Laboratory (LBNL) had to be abandoned due to detector activation arising most probably from passive beam shaping contaminations. The dual-head PET BASTEI (Beta Activity Measurements at the Therapy with Energetic Ions) that has been installed at the GSI pilot project has demonstrated its ability to provide a control of neck and head irradiations with carbon ions. Nevertheless, improvements of this prototype were required to cope with:

- More delicate therapeutic situations (geometry optimisation)
- Recent accelerator developments implementing optimised beam extraction techniques result in much reduced timing window for in-beam PET data taking if the presently installed acquisition technique is applied (DAQ improvements)

The technical constraints of an in-beam PET are the followings:

- fast accessibility of the medical personnel to the patient at all times;
- collision-free solution concerning in-beam PET, beam nozzle and patient and couch;
- collision-free solution concerning in-beam PET and the incoming and outgoing particle;
- volume minimised tomography due to integration reasons;

2.1 Introduction

The PET BASTEI is a dual-head prototype for three reasons:

- to avoid the activation of the detectors with good security margins,
- to respect the patient positioning restrictions imposed by the fixed and horizontal beam line,
- because the preliminary studies performed showed that a dual-head PET should be accurate enough for the small-sized tumours that were first planned.

This PET BASTEI consists of two detectors heads with $42 \times 21cm^2$ front area each. Each head was built with detector blocks of BGO coupled to photomultiplier tubes (PMT) from the ECAT EXACT tomograph from CTI PET Systems Inc. A total of 8×4 scintillation block detectors were implemented in each head, with each detector block consisting of 8×8 BGO crystals with $54 \times 54mm^2$ front surface each (centre-to-centre) and $2cm$ depth, read by four PMT. The PET data, acquired and saved in list mode format, are submitted to a dedicated, attenuation-correcting, maximum likelihood expectation maximisation algorithm MLEM with a correction for single Compton events occurring in the object. This algorithm allows to reconstruct the measured β^+-activity in the patient. Visualisation is done by merging the in-beam PET images with the patient CT.

2.2 Geometry optimisation

The influence of the HadronPET (e.g. PET dedicated to hadrontherapy) configuration on the image quality has been studied in detail within [1]. The main parameter that determines the image quality is the gap between the dual heads. Figure 2.1 shows the scheme of the dual-head PET studied and defines the angle that determines the two gaps between the dual-heads.
This study relies on two-step simulations:

- First, list mode data sets are produced by a simulation that can consider ring detector arrangements as well as any camera with two gaps.
- Second, a routine based on maximum likelihood expectation maximisation algorithm (MLEM) read the list mode data provided by the first step.

2.2.1 Dual-head PET

On the figure 2.2 we see that the reconstructed images obtained with wide gaps $= 100^o$ show the expected object elongation along the Y_{PET} axis.

Figure 2.3 depicts a typical portal for a head and neck irradiation with carbon ions. The images on the top row show the delivered physical dose generating a given β^+-activity distribution, shown in the bottom row. Both the physical dose and the β^+-activity distribution are superimposed onto the CT of the patient.

Figure 2.4 shows the reconstructed images of the simulated β^+-activity distributions obtained with the three different detector geometries. Theses images has been obtained with an β^+-activity one order of magnitude higher than the estimated target activity produced in treatment. This was done in order to study the influence of the detector geometry without influences of low statistic data sets.
The images obtained with the closed ring tomograph are remarkably similar to the β^+-activity distribution displayed in figure 2.3. This was expected since, despite the rotation of the camera in respect to the beam direction, the field of view (FOV) of the camera covers all the irradiated volume.

In what concerns the images obtained with dual-head camera, we can see that the quality of the reconstructed images shown seems to be quite high for moni-

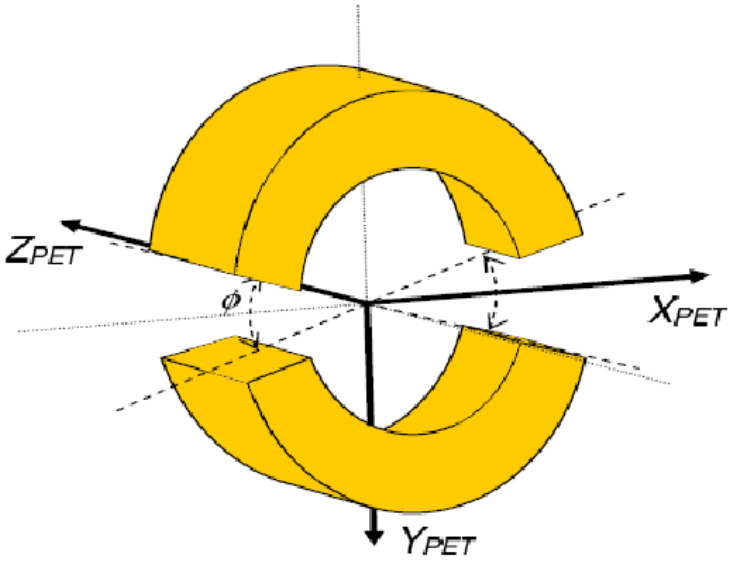

Figure 2.1: Scheme of the dual-head positron camera studied. The gap between the two detector heads defines the angle θ at the isocenter, with $\theta = 0^o$ representing a closed ring camera.

toring small tumour irradiation if the gap between heads is not to big.
The same kind of study has been performed with:

- more realistic, **low statistics** simulations: despite the higher noise (granularity) of the images, the agreement of the remaining iso-activity lines with the simulated, deposited activity is still valid.
- **large irradiation fields** occurring during tumor treatments in the pelvis region: in-beam PET clearly requires closed-ring tomography.

2.2.2 Closed-ring PET

Due to the higher image quality obtained with a closed-ring tomograph, particularly with large irradiation fields, the possibility of implementing such an in-beam PET scanner for heavy ion tumor irradiation has been investigated. Figure 2.5 depicts a worst-case irradiation scenario: a beam portal with maximum beam width and delivered perpendicularly to the patient.

The conclusion is that tomograph with e.g. a radius $R_{PET} = 45,8cm$ and axial FOV $a = 24cm$ can be implemented with a patient table not wider than 65 cm (the maximum width at the GSI facility) provided that the distance between the nozzle and the isocenter is not smaller than 50cm.

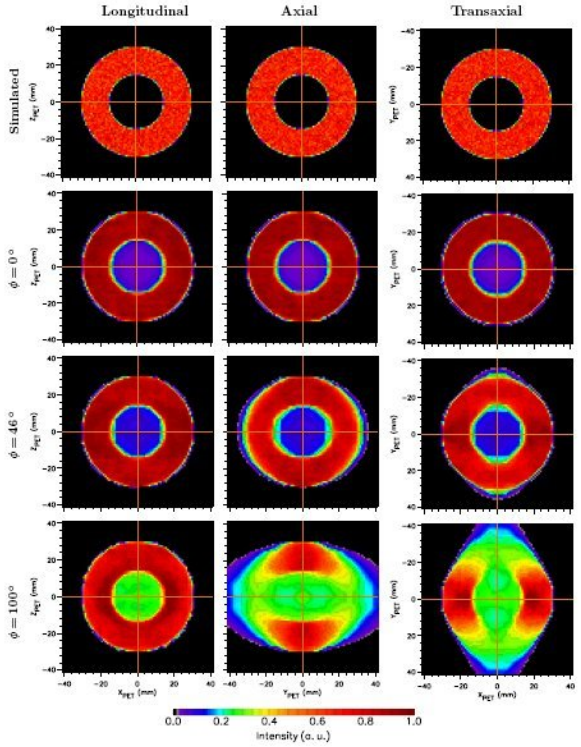

Figure 2.2: Image deterioration with dual-head tomographs. The imaging of a hollow sphere filled with a homogeneous activity of $1MBqcm^3$ and positioned at the centre of the FOV of three different tomographs was simulated. The top row shows the simulated spatial distribution of the annihilating events. In the three following rows, reconstructed images of the events detected with a closed-ring detector configuration (16 million events detected), a dual-head geometry with $\phi = 46^o$ (11 million) and with $\phi = 100^o$ (6 million events detected) are displayed.

2.3 Integrating In-beam PET

2.3.1 PET at a fixed, horizontal beam line

It is similar to the present implementation of BASTEI in the sense that the mechanical structure holding the two PET detector heads moves along the beam nozzle, bringing the tomograph into the measuring position and back. The main difference lies in the capability of rotating each detector head about a vertical axis, therefore allowing the tomograph to be placed at the isocenter in a tilted position with respect to the incoming beam. Two configurations are possible:

- a closed ring positron tomography:
  the rotation along the vertical axis of the mechanical arms holding the two detector heads allows a closed ring positron tomograph to be installed if the dimensions detailed in the previous section are taken into account.

- a dual-head tomography with small gaps.

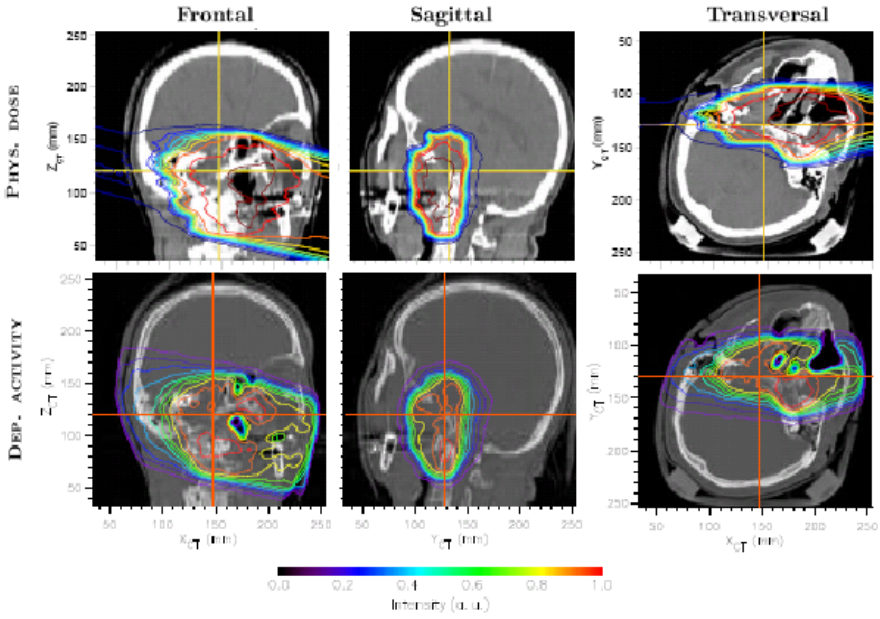

Figure 2.3: Head and neck irradiation: top row show the delivered physical dose generating a given activity shown on bottom row.

Besides, in the case of an emergency, the heads just need to be moved apart vertically.

2.3.2 PET at the patient couch

In this configuration, the tomograph is installed with its rotation axis parallel to the patient table. The dual-head PET scanner moves along the couch and can be positioned around the region being irradiated, with the aperture between the two detector heads allowing the beam to pass through without touching the γ-ray detectors. A closed ring tomograph can also be considered by tilting the detector heads around an axis perpendicular to the beam direction. Nevertheless, the most important disadvantage of this configuration is the forbidden irradiation area in the cranio-caudal direction arising from the interaction of the particle flux leaving the patient with the support of the PET scanner.

2.3.3 PET on a Separate Gantry

If the PET scanner is fixed on a separate gantry, positioned inside the treatment room and opposite to the patient couch, then all positions of the PET become available. However, the positioning of the positron tomography requires an extra coordination of several synchronous movements that may lead to physical collisions in the case of machine or human error.

This item constitutes the main disadvantage of the present configuration, together with the time required to gain access or release the patient being treated in the case of an emergency.

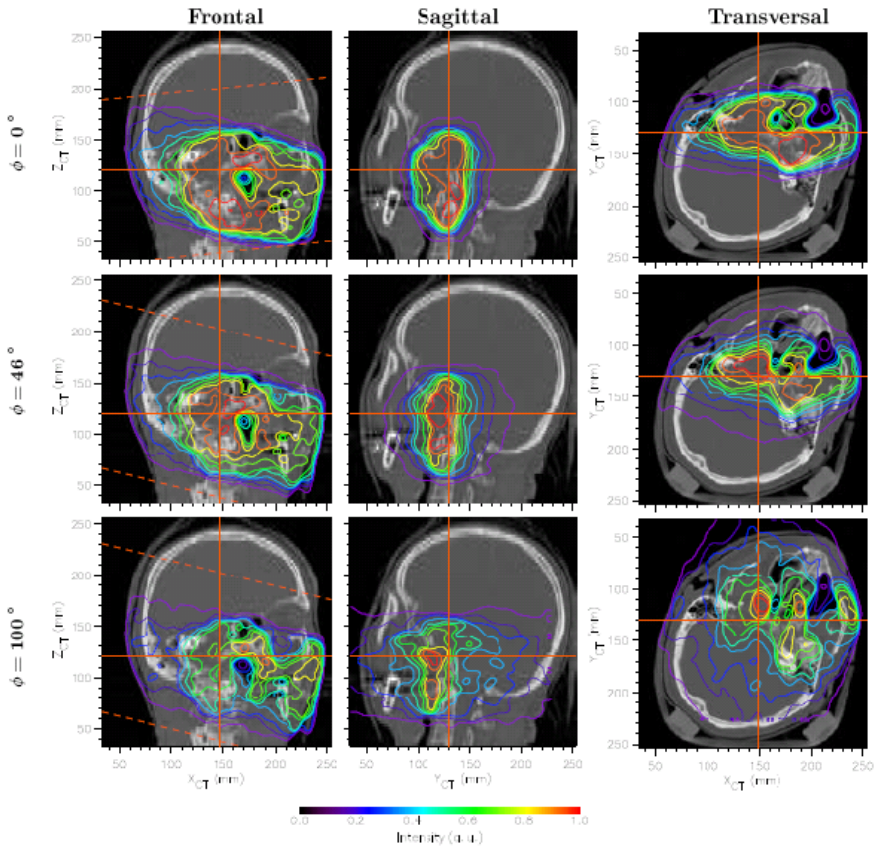

Figure 2.4: Head and neck irradiation: reconstruction with different tomographs. [1]

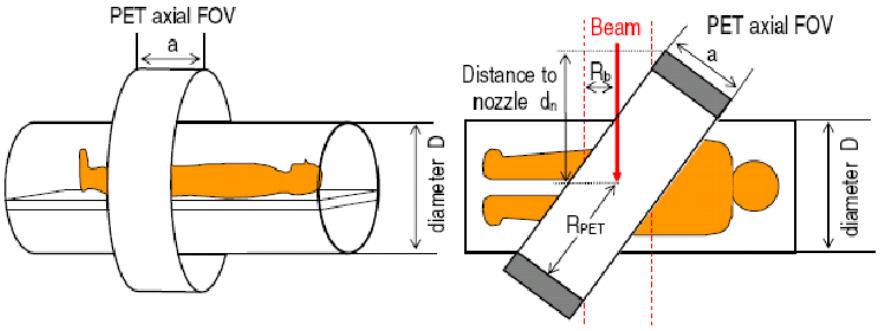

Figure 2.5: Scheme of a closed-ring, in-beam PET tomograph with inner radius RPET

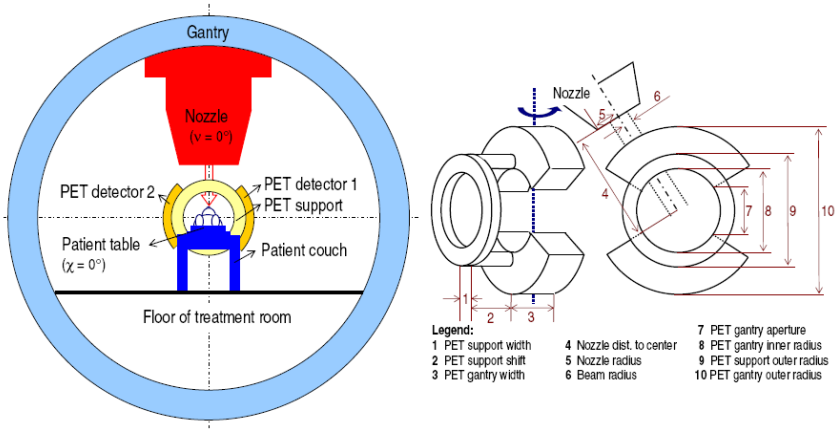

Figure 2.6: PET at the patient couch. A dual-head positron scanner is fixed to the patient couch with its axis parallel to that of the patient table. The detector heads rotate, based on their support ring, allowing the aperture between them to be positioned along the beam (not shown in the right image).

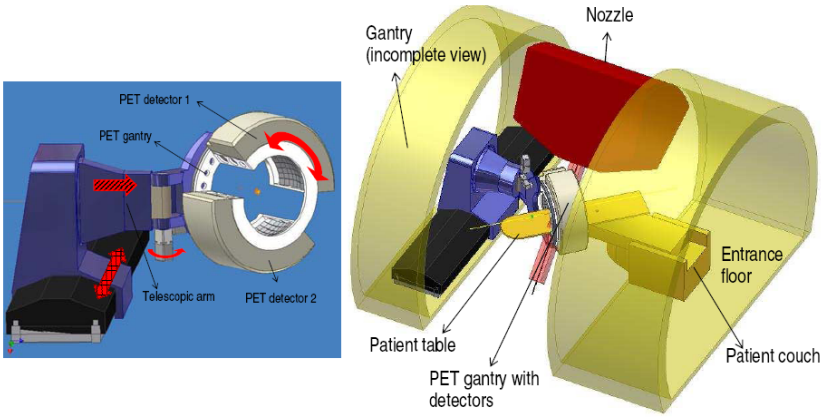

Figure 2.7: PET on a separate gantry. A dual-head positron scanner is fixed on a separate gantry, positioned inside the treatment room and opposite to the patient couch. The patient is first positioned for treatment, followed by the positioning of the dual-head scanner with movements indicated with the block arrows in the left image

2.4 Off line, off beam PET

It has to be mentioned that off-line PET is still investigated in the German hadrontherapy centres [2] . Indeed, this PET choice allows the use of commercial ring tomographs which are widely used for PET tracer imaging. However, the applicability and usefulness of off-line PET monitoring is limited to the detection of the long-lived isotopes. Furthermore, the moving of the patient from the treatment site to the PET scanner after irradiation may introduce additional position uncertainties. Hence, new off-line strategies are investigated, e.g. using PET/CT instead of PET imaging alone, using the same patient positioning system for irradiation and PET measurement and moving the patient without realease from the positioning system to a scanner installed as close as possible to the treatment site.

Chapter 3

Detectors

The detector part of a PET camera is one of the most important factor involved in image quality.
In the context of in-beam PET, the characteristics that we will need for those detectors are the following:

- high detection efficiency for annihilation radiation
- a fast scintillator enabling the smallest time resolution for the suppression of random coincidences (essential for in-beam PET readout during beam extractions)
- good energy resolution for rejecting Compton photons scattered in the patient
- insensitivity against influences from the therapy beam : their imaging capability is expected to be mostly influenced by the particle and photon flux generated by nuclear reactions
- hardness against hadronic radiation
- magnetic field insensitivity : the acquisition would be operated close to the last magnet of the rotating medical beam line. Conservative calculations of the fringe magnetic field expected outside the mentioned magnet, show that the presently used photomultiplier tubes do not provide enough magnetic field resistance, even when covered with an optimum magnetic field shield such as mu-metal sheets
- compactness, to have flexibility for positioning the patient at the beam delivery, this includes spatial restrictions due to the number of diagnostics instrumentation to be installed at the patient treatment site
- a fast signal processing and data acquisition able of separating the events acquired during the high rates registered during particle extractions

3.1 Scintillators

3.1.1 Detector Development: LSO Scintillator coupled to APD Arrays

The in-beam positron emission tomograph at GSI Darmstadt is based on PET technology for tracer imaging available at the time of installation. Consequently, its radiation detectors, scanner geometry, data acquisition and processing are suboptimal with respect to the requirements of next-generation, in-beam PET systems for therapy monitoring at future heavy ion clinics.
For instance, for the new scanner to be installed at the dedicated heavy ion facility in Heidelberg the γ-ray detection material BGO is planned to be substituted with a state-of-the-art, commercially available scintillator that better satisfies the requisites mentioned. One possible candidate is cerium-doped lutetium oxyorthosilicate (Lu2SiO5:Ce3+, LSO).

3.1.2 Additional prerequisites for an in-beam PET scintillator

In addition to the main scintillator properties required when used in nuclear medicine imaging with PET, the requirements of in-beam PET include also a radiation hard crystal that does not become activated, leading to γ-ray lines in the 511 keV region. This is necessary due to the light particle flux consisting mainly of neutrons and protons, but also with slightly heavier particles, that has been measured to leave the irradiated patient downbeam, peaked in the forward direction.
All crystal scintillators suffer from radiation damage when exposed to large radiation doses. The most common damage phenomenon is the appearance of radiation-induced absorption bands caused by colour centre formation. The absorption bands reduce the light attenuation length of the crystals and, consequently, its light output. Other effects include an increase in phosphorescence (afterglow), which leads to an increase in readout noise, and a reduced intrinsic scintillation light yield due to damage of the scintillation mechanism. This is to be taken into account when looking for new scintillators.

It has been shown that LSO is a fairly radiation hard scintillator up to 100 kGy, and experience at GSI seems to prove that this cristal would be apprpriated for an on-line in beam PET.
Due to its short decay constant, a time resolution of 1.2 ns has already been achieved in a commercial PET scanner (with BGO-based tomographs presenting typically 12 ns). Therefore, renewed interest in taking advantage of the time-of-flight information in LSO-based tomographs has arised. (Note: LYSO TruFlight, Gemini Philips 650 ps)
One must notice that an other important characteristic that has to be taken into account is the intrinsic activity of the crystal. In [1], it is shown that the intrinsic true coincidence rate arising from the natural background activity of Lu in LSO does not influence significantly in-beam PET images acquired with BASTEI, with the random suppression technique used. For a next-generation, closed ring or dual-head tomograph one must be able to efficiently suppress the intrinsic random coincidences, either by signal processing or by reducing the

coincidence time window (which means to improve time resolution).

3.2 Photodetectors

The gamma rays emitted by positrons are turned into visible light by the scintillators, the photodectectors must then detect efficiently this visible light.
The characteristics that one will expect of a good photodetector are:

- Good spatial resolution
- Low cost per unit area
- High quantum efficiency and gain
- High speed
- High dynamic range
- Good linearity
- Minimal dead area

So far, most of the clinical PET use photomultipliers tubes (PMT) as photodetectors, their main advantage being their high gain. But PMT are sensitive to a magnetic field of the order of those expected at the end of the beam, and so could not be used in hadrontherapy environment.
Avalanche photodiode arrays (APDA) fullfill the requirements of magnetic field insensitivity and spatial restrictions. They have been already studied and tested by different teams and seem to be a good solution for future in-beam PET detectors.

Chapter 4

Data processing

The data acquisition system development cannot be disconnected from the development of the rest of the system. Quick and efficient detectors mean also important flux of data to collect quickly.

4.1 Data acquisition

Ion beams are not continuous and the temporal structure is a crucial point for the data acquisition system. At GSI, the data acquisition has been setup to avoid the high random event rates occurring during the extraction of the ions. First the macro structure ($\sim$ a few seconds) was used to veto the events occurring during ion extraction. Then the method has been refined, using the microstructure ($\sim$ a few ten nanoseconds) to get extra data with a number of random coincidences as low as possible.

4.2 Dedicated reconstruction algorithm for in-beam PET data

4.2.1 Introduction

In order to improve in-beam PET by optimising the detector geometry and position, a versatile simulation and reconstruction software package was necessary. Therefore, to the fully 3D, re-binning-free, MLEM algorithm developed for BASTEI, a histogram factorisation method was added for allowing the MLEM algorithm to be applied to several closed-ring or dual-head tomographs with variable dimensions.

4.2.2 Reconstruction of list mode PET data

System symmetries and factorisation algorithm implemented

A set of simulation and reconstruction routines capable of handling a high number of coincidence channels, corresponding to a high resolution, closed-ring or dual-head tomograph, was developed. Considering, as an example, the ECAT

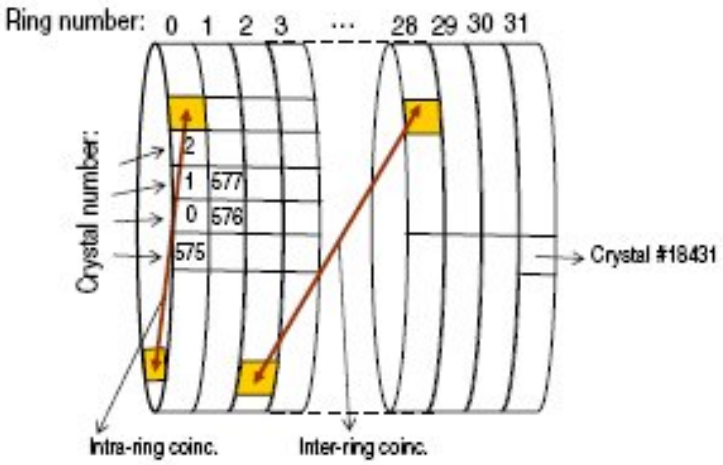

Figure 4.1: Intra- and inter-ring coincidences and ring and crystal numbering adopted for the reconstruction routine. A closed-ring detector geometry is illustrated. If a dual-head tomograph is considered, crystals that are absent are simply ignored.

EXACT HR+ tomograph from CTI PET Systems Inc., containing 32 complete detector rings, the total number of crystals is 18432.
Since in-beam PET is characterised by low-statistics data sets sampled with a limited-angle tomograph, re-binning the 3D collected data into 2D sets disturbs the spatial information of the few LOR existing, which forbids the application of already existing re-binning algorithms. Therefore, a fully 3D implementation of the MLEM algorithm was developed by making use of the system symmetries and coincidence channel possibilities illustrated in figures 4.1 and 4.2.
Figure 4.1 shows the crystal numbering scheme implemented both in the simulation and in the reconstruction routines. For every detected coincidence, the simulation registers, in list mode, two numbers corresponding to the crystal hits. It is up to the reconstruction routine to histogram the incoming list mode data appropriately before proceeding with the iterations of the MLEM algorithm. In order to handle the enormous amount of crystal combinations possibilities (approximately 170 million), dynamic memory allocation was necessary together with a factorisation scheme that allowed the reconstruction to handle only non-empty coincidence channels. For that, all possible coincident crystal combinations were analysed following the scheme in figure 4.2.

4.2.3 Time-of-flight reconstruction of real treatment simulations

During heavy ion treatments, a considerable amount of activity is transported to locations outside the FOV of the in-beam positron tomograph. In these situations, the use of TOF information may decrease the number of background events registered. But the most important advantages of an eventual in-beam TOF-PET arise if the time difference between the arrival of the photons is used to directly compute, on an event-by-event basis, the location where the positron

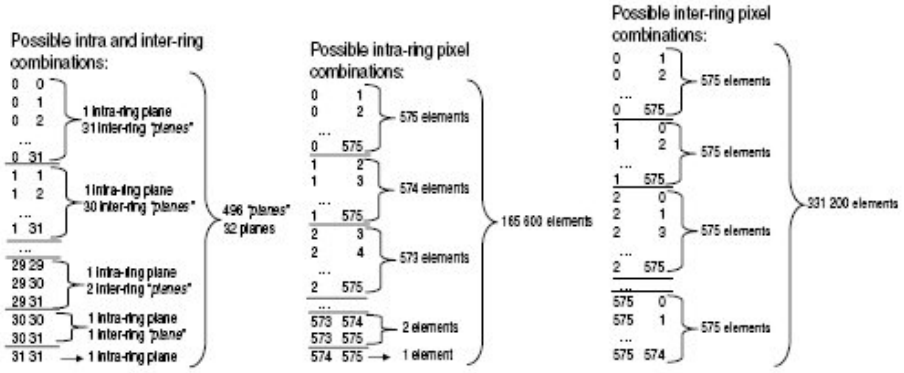

Figure 4.2: Scheme showing possible intra-ring, inter-ring and pixel combinations.

Treatment	Image size (cm^3)	Number of events	Run time	
			TOF[a]	MLEM (50 iterations)
Head and neck	$22 \times 20 \times 20$	1.3×10^6	45 s	5 h 40 m
Pelvis	$40 \times 25 \times 25$	5.3×10^6	103 s	$>$ 5 days

[a] The image is ready after a single iteration through the data

Figure 4.3: Comparison of times required for image availability: direct-TOF (a single iteration is performed through data) versus MLEM-based PET imaging. Computations executed on an Intel(R) Xeon(TM) CPU 3.20 GHz dual-processor. All reconstructions regard a dual head tomograph with wide gaps ($\phi = 100^o$).

annihilation occurred. Not only the computing time is immensely reduced, as shown in the table of figure 4.3, but also the limitations arising from limited-angle tomography vanish if the coincidence time resolution is better than 200 ps FWHM (which leads to about $\pm 3cm$ spatial resolution).

The most impressive results expected if TOF-PET detectors with very high coincidence time resolution (below 200 ps FWHM) would be commercially available, are the speed with which the image becomes available to the radiotherapist after the irradiation of each portal: below 2 minutes as demonstrated in the table of figure 4.3. This increase in image processing speed arises from the possibility to calculate at once the point of positron annihilation as soon as the coordinates of the hit detectors and the TOF information are known. Such algorithm needs to process one single iteration through the collected data only, in opposition to the 50 iterations necessary with the MLEM algorithm which, in addition, needs to cross the full image space for every pair of detectors that was triggered. Due to this last detail the processing speed of the direct TOF algorithm is expected to stay below that of fast, expectation maximisation algorithms like OSEM.

The time to obtain an image is already smaller than the typical irradiation time, with improved reconstruction computing facilities TOF-PET would allow

the image to be processed and shown to the oncologist during the course of the irradiation, i.e. in-beam PET could be called for the first time on-line, in-beam PET.

Part II

Next challenges

Chapter 5

In-beam and on-line (?) PET

5.1 Detectors

5.1.1 Scintillators

There is a variety of radiation detection applications that require scintillators with high light output, good attenuation power, and a low level afterglow, but absolutely needs a fast scintillator decay time. This is particularly true for HadronPET. The next table, from [1], summarises some properties of a large panel of scintillators that have been or are currently of interest in nuclear imaging. Among all, there is a new crystal for which the PET research community shows deep interest: LaBr3:Ce. Because LaBr3 have better luminosity and short decay time, it holds promise for improving PET detection, but would require sacrificing spatial resolution in order to obtain better energy resolution and TOF capability. Recent studies with simulated 3D whole body scanner based on LaBr3 Anger-logic detectors, have achieved a 300 ps timing resolution [3]. They have also shown, in the conditions, that using LYSO crystal(similar to LSO), the coincidence timing resolution is about 600ps.

5.1.2 Photodetectors

We have seen that PMTs, so far widely used are likely to be remplaced by APDA for future PET. However, some other promising new photodetectors also exist and might be investigated in the context of hadrontherapy control instrumentation. They are, for instance:

- MA-PMT : Multi-Anode PMT
  This pixelised photodetector has been used for instance in the small animal PETs of the ClaerPET collaboration. They have high gain but are not as compact as APDA, and are magnetic field sensitive.
- Si-PMT : Silicon Photomultiplier Tubes
  As mentioned in [4], the SiPM is a solid state photodetector, which consist of a multipixel semiconductor photodiode. For Medical Science applications, the most attractive feature of the SiPM are its insensitivity to

Scintillator	Density ρ ($\mathrm{g\,cm^{-3}}$)	ρZ_{eff}^4 ($\times 10^6$ $\mathrm{g\,cm^{-3}}$)	Atten. length[a] (mm)	Photo effect fr.[a] (%)	Hygro-scopic	Yield (ph./ keV)	Decay const. (ns)	Peak emission (nm)	$\Delta E/E$[b] (%, FWHM)	dE/dx per mip[c] (MeV/cm)	After-glow (%/ms)	Medical application	Reference(s)
NaI:Tl	3.67	24.5	29.1	17	Yes	41	230	410	5.6	4.8	0.3-5/6	SPECT	[Hof48, Sho84]
CsI:Na	4.51	38	22.9	21	Yes	40	630	420	7.4	5.6	0.5-5/6	XII	[Hel00]
CsI:Tl	4.51	38	22.9	21	Slightly	66	>800[d]	420	6.6 4.3[e]	5.6	0.5-5/6	SPECT, PET, CT	[vE02, Gar00]
CsF	4.64	37	20.0	23	Very	2 2.8	3 5	390		6.0[g]		TOF-PET	[Mos83]
BaF_2	4.89	42	20.5	17	Slightly	2[f] 8.2[s]	0.7[f] 620[s]	220[f] 310[s]	10	6.6		TOF-PET	[Lav83]
BGO ($Bi_4Ge_3O_{12}$)	7.13	227	10.1	40	No	9	300	480	9.0	9.2	0.005/3	PET	[Web73]
LSO (Lu_2SiO_5:Ce)	7.4	143	11.4	32	No	26	40	420	7.9	9.7[g]	$<0.1/6$	PET	[Mel92, Mel91]
LYSO $\frac{\mathrm{Lu}}{\mathrm{Y}}$ ($Lu_{1.8}Y_{0.2}SiO_5$:Ce) $\frac{90}{10}$	7.1	127	11.5		No	26[h]	41	420	7-9	7.8[g]	$<0.1/6$	PET	[Coo00, Pid03]
($LuYSiO_5$:Ce) $\frac{50}{50}$	6.0	75	16.7	21	No	26[h]		420	7-9	7.1[g]	$<0.1/6$	PET	[Kim02, Mos99b]
LuAP ($LuAlO_3$:Ce)	8.3	148	10.5	30	No	12	18	365	~ 15	11.0[g]		PET	[Min94, Mos95]
LPS ($Lu_2Si_2O_7$:Ce)	6.2	103	14.1	29	No	30	30	380	~ 10	8.3[g]		DOI-PET	[Pau00]
LGSO ($Lu_{0.4}Gd_{1.6}SiO_5$:Ce)	6.5	79	14.3	26	No	16	65	440	8	8.6[g]		PET	[Shi04]
GSO (Gd_2SiO_5:Ce)	6.7	84	14.1	25	No	8	60	440	7.8	8.7[g]		PET	[Tak83, vE02]
YAP ($YAlO_3$)	5.5	7	21.3	4.2	No	21	30	350	4.3	7.8[g]			
$LaCl_3$:Ce	3.86	23.2	27.8	14	Yes	46	25 (65 %)	353	3.3	5.2[g]		SPECT	[vL00]
$LaBr_3$:Ce	5.3	25.6	21.3	13	Yes	61	35 (90 %)	358	2.9	6.9[g]		SPECT	[vL01]
$CeBr_3$	5.2	26.6	21.5	14	Yes	68	17	370	3.4	5.9[g]		TOF-PET	[Sha04]
LXe (liquid xenon)	3.06	26	30.4	21	-	11 26[j]	27 (30 %) 45 (70 %)[j]	165	22/16[i]	3.9[g]		DOI-PET	[Che83]
$PbWO_4$	8.2	268	8.9	43	No	0.2	15	440-500		13.0			[Sch92, Cry00]
Plastic (vinyltoluene)	1.03	<0.005	444	-	No	<12	1-3	375-435	-				[Paw95, Bir64]
Ideal (PET, PMT)	>6	>245	<12	>30	No	>8	<500	300-500	<10	-			[Der82, Mos00]
Ideal (PET, APD)						$\gg 8$		400-900					
Ideal (TOF-PET)						$\gg 8$	<40						

[a] At 511 keV.
[b] At 662 keV, PMT readout.
[c] Minimum ionizing particle.
[d] Smaller than 6 μs.
[e] At 662 keV, PMT and silicon drift detector (SDD) readout.
[f] Fast decay component.
[g] Extrapolation from $Z_{eff}/A \times \rho$, based on NaI.
[h] PMT readout, 33 ph./ keV with APD readout.
[i] At 511 keV, with 22 % in [Che04a], 16 % in [Cre00] (ionization mode).
[j] Arises from e^-/ion^+ recombination, vanishes under electric field.
[s] Slow decay component.
SPECT: Single photon emission computed tomography.
XII: X-ray image intensifier.
TOF-PET: PET with time-of-flight information.
DOI-PET: PET with depth-of-interaction information.

Figure 5.1: Detection of γ-rays in Nuclear Medicine Imaging

magnetic field, its high photodetection efficiency (up to $\sim$ 70%) and its comptactness but there are many other advantages, such as the low bias voltages, the very high gain of 10^6, the low power consumption, etc... At present, the major problems of SiPMs are the cross talk between micropixels in the SiPM, the high dark current and for the PET application their small size.

- MCP-PMT : Microchannel Plate Photomultiplier Tube
  Microchannel Plate Photomultiplier Tube are photomultiplier tubes in which the electron amplifier part consist in microchannel plates. This makes them insensitive to magnetic field, they also have a very good gain (typically 10^6), and their quantum efficiency is around 20%. They can offer an extremely good time resolution : resolution as good as 30 ps has been reported in [5]. One major concern about those detectors are their life time. Aging studies like reported in [6] show that the lifetime can be improved by using a protection layer to reduce the ion-feedback that causes early aging.
  Some tests have also been made at CERN for the CNAO[1] on a Burle prototype [7]. The ion-feedback aging is planned to be reduced at CNAO by swiching on the high voltage only during the real acquisition phase i.e. during ions spills. However, the aging of the detector with the high voltage off but staying near the beam still must be studied carefully.
  Other attempts have also been done to use microchannel plates directly without any photocathode, with an illumination perpendicular to the axe of the microchannels. This is called "edges-on" illuminated MCP. It has been shown in [8] that this method can be used to image a source of ^{137}Cs, emitting 662 keV photons, however it remains more usable for X-rays than for gammas.

- Gaseous detectors
  Gas-filled detectors of particles have the advantage of low cost and good statial resolution. For 511 keV gammas, high Z material foils must be used as converters inside the gas, this leads to degradation of the energy resolution. First gas detectors used in medical environement where wire chambers they have the disadvantage to be quiet fragile. Resistive Plate Chambers (RPC) and Gas Electron Multipliers (GEM) are the gas detectors that could be used for PET. Their low detection efficiency could be compensated by an increase of the axial field of view (their low cost permitting a full body coverage), but for in-beam PET the detection efficiency is an important issue as well as the compactness, in these conditions its seems difficult to take advantage of the RPC and GEM while there efficiency has not been seriously increased. Researches are on going on this subject in different teams [7].

[1] Italian Centre for Oncological Hadrontherapy

5.2 Data Processing

5.3 Data acquisition

Concerning data acquisition, the first question is "Does is worth to try to achieve a real-time PET?"
The advantage of having such an imaging system is kind of obvious : the imaging system could then, in principle, be linked to the irradiation system as a feed back loop control and in this way be able to correct in-line any dose deposition. This would avoid to have to re-plan the treatment for the following sessions, or in case of an unique session. First the electronics must run real-time and this means not only quick but also without any dead time. Then, not only the imaging system should be run in real time, but the full comparison of the planned dose deposition at any instant with actually measured dose should be done on-line. The current reconstruction codes are far from being runable in real time.
It is clear that a real-time in-beam PET camera would be the dream's instrumentation to avoid any trouble in dose delivery but so far it seems a bit difficult, more detailed technical studies both on electronics DAQ and on reconstruction codes should be done to have a clue on the feasibility.

5.3.1 Counting rates

In the perspective of on-line PET, one very crucial point to address is the instantaneous count rate that is to be expected. One must have enough data instantly (in a short time) to reconstruct a good image, but rates should also be low enough to avoid events pile up.
Some tests have been made at GSI using new generation detectors (i.e. LSO/APDA) and the setup shown on figure 5.2. This PET prototype is made out of two detectors LSO/APDA that each consists in $8 \times 4 = 32$ LSO crystals ($2.1 \times 2.1 \times 15 mm^3$ each) coupled individually to 4×8 pixels of a Hamamatsu S8550 APDA. The electronics used consists in dedicated low-noise pre-amplifiers that read the APDA then followed by standard nuclear physics modules.
The irradiation time was 20 minutes long (standard irradiation time), with a beam structure of 2 seconds of extraction and 3 seconds of pause. The C-12 beam size was 3.7 mm diameter (FWHM), with an energy of 341.9 MeV/u. The beam intensity was 2×10^8 ions per spill with 1400 spills for each irradiation, which yields to a fluency about 1 000 times higher than for a typical daily treatment fraction (3×10^8ions).
With a detection threshold of 250 keV, the counting rate of coincidence events above the threshold are shown in the following table (singles rates are not known for this experiment since the acquisition was triggered by the coincidences detection).

	coincidences
during extraction	652Hz
during pauses	20Hz

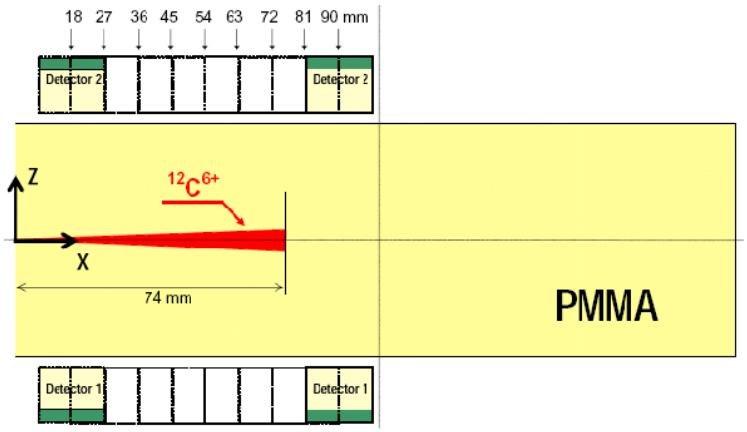

Figure 5.2: Setup used for some of the tests performed at GSI for in-beam PET. Fantoms were irradiated in order to image the β^+-activity resulting from stopping carbon ion beam. the distance between the centre of the fantom and the detector was 56 cm.

This is comparable, in terms of order of magnitude of counting rates, to what as been measured at GANIL with the setup described in Chapter 7. Correcting for the beam intensity and the detection geometry differences, the gamma prompt counting rates (with the same 250 keV threshold) are the following:

	singles	coincidences
during extraction	2200 Hz	200Hz

One can see that those counting rates, event during ions extraction seem quite manageable with the kind of electronics and DAQ developed for particle/nuclear physics today.
More detailed studies are being carried on (in particular Geant4 simulatios) for the quantification of the expected rates (especially singles counting rates). This will allow the estimation of the integration time necessary, in these conditions, to have a good image, and in this way to have a first clue on the theoretical feasibility of a real-time in-beam PET camera.

Chapter 6

In-beam detector

Particle detectors for beam diagnostics are currently used on active beam shaping systems of hadrontherapy facilities to control the position of the beam typically each $100\mu s$. Its association with ionisation chambers that measure the beam intensity is the heart of the fast control system installed. The layout of the beam diagnostics has to obey important characteristics, concerning the precision of the devices, their usability, as well as their operational availability.
In the frame of the treatment control with a PET tomography, these particle detectors can play an important role for two reasons that will detailed in the following paragraphs.

6.1 Beam structure and data acquisition

A synchrotron beam presents both time macro- and micro- structures :

- Macrostructures correspond to the cycle of the accelerator, namely the filling of ring and the ion acceleration (during which no ions are launched on the patient) and the beam extraction. Theses steps in the accelerator cycle typically last several seconds.
- Microstructures are due to a correlation between the moment of arrival of the carbon ions and the phase of the RF-signal. The period of the RF-signal is of the order of several hundreds of nanoseconds whereas the ion arrival last about a few tens of nanoseconds.

During the moment of arrival of the carbon ions, the high rates of prompt radiation (mainly gamma rays and neutrons) are responsible for random coincidences that cannot be suppressed with random-correction techniques from conventional PET. That is why the data acquisition of the PET BASTEI was performed between the beam extractions. This data acquisition has been improved within the PhD work of Crespo: two methods for suppressing the micropulse-induced random coincidences have been proposed.

6.2 Suppression of random coincidences during particle extraction

The first method consist in storing the coincidences detected with the positron camera in correlation with the phase of the RF-signal. The events occurring within the ion arrivals can either be labelled for posterior elimination or immediately discarded by the acquisition electronics (DAQ). A second method of labelling coincidences arriving during the microbunches makes use of a thin, fast particle detector (FD) placed in the beam path in front of the target. In principle, this approach (also called the $\gamma\gamma - ion$ method) should allow the implementation of narrower time windows around the ion arrival when compared to the RF-method. The $\gamma\gamma - ion$ method is easier to implement in real therapeutic situations since it does not require a correction for the transit time of the ions in the beam pipeline (which is dependent on beam energy). Nevertheless, its has the drawback of requiring additional material in the beam path unless the fast particle detector could be used also as a beam monitor, which is not a trivial task since a large area, position sensitive detector covering the whole beam delivery portal ($20 \times 20 cm^2$ at GSI) would have to be assembled. In addition, the very high mean number of particles per bunch (typically 10^3) for proton treatments requires the eventual beam monitor to be able of performing charge integration in order to detect ions overlapping in time. In summary, an ultra-fast, particle counter detector with a large dynamic range would be required, which is indeed a technological challenge.

6.2.1 Correlation between $\gamma\gamma$ detection and time of ion arrival

Besides, if the fast position sensitive detector had a time resolution of the order of the nanosecond, it could be possible to tag each arrival of the ions. Then, this time label could be taken into benefit to improve the image reconstruction: indeed, the spatial and time correlation between the ion crossing through the particle detector and the detection of the following lines of response could allow to :

- suppress a lot of background events due to the considerable amount of activity transported to locations outside the FOV of PET,
- bring an additional information that could speed up the time of image reconstruction.

Simulations of irradiation and image reconstruction are required to evaluate the interest of this technique.

Chapter 7

Gamma prompt monitoring

Besides PET, prompt radiation detection may be regarded as a promising technique to control the dose during ion irradiation treatments. Indeed, within less than a nanosecond following the ion beam impact, and neutrons are emitted by excited nuclei with very high statistics each time nuclear fragmentation occurs. Thus prompt radiation may be used as a monitor of the dose inside a patient, provided fragmentation probability along the path is well known. Moreover, the emission profile of prompt radiation is somewhat correlated to the primary beam range, since fragmentation occurs along this path. Thus, not only the total dose could be measured, but also its longitudinal distribution. Technically, this implies to be able to discriminate radiations coming directly from the ion track from those scattered in the surrounding matter, namely elastically- and inelastically-scattered neutrons and Compton-scattered gamma. Recently, Min et al.[9] studied the longitudinal distribution profile of prompt gamma following proton impact in thick targets, using a collimated scanner detection setup. They found that information on the ion range is kept even for energies up to 200 MeV.
Collaboration between a group of the IPNL institute and 2 groups of the INSA extends this work to carbon ion beams, for which projectile fragmentation occurs in addition to target nucleus fragmentation. A first experiment has been performed in June 2007 at GANIL on a beam of 73 MeV/u carbon ions. The main goal of this experiment was to demonstrate the correlation between the ion path in the matter and the depth profile of the prompt gamma emission. Figure 7.1 shows one of the experimental configuration on which one can see :

- the scintillator NaI (Tl) collimated along a direction perpendicular to the beam direction
- a PMMA target placed on a table allowing its translation along the beam direction
- a shielding to reduce the detection of neutrons and gamma rays scattered in the experimental area

In particular, this group improves the detection technique by using combined time of flight and energy discrimination between gamma rays and neutrons. The first results obtained during the experiment performed at GANIL in June 2007 are very promising (an article will be submitted within the next month), namely

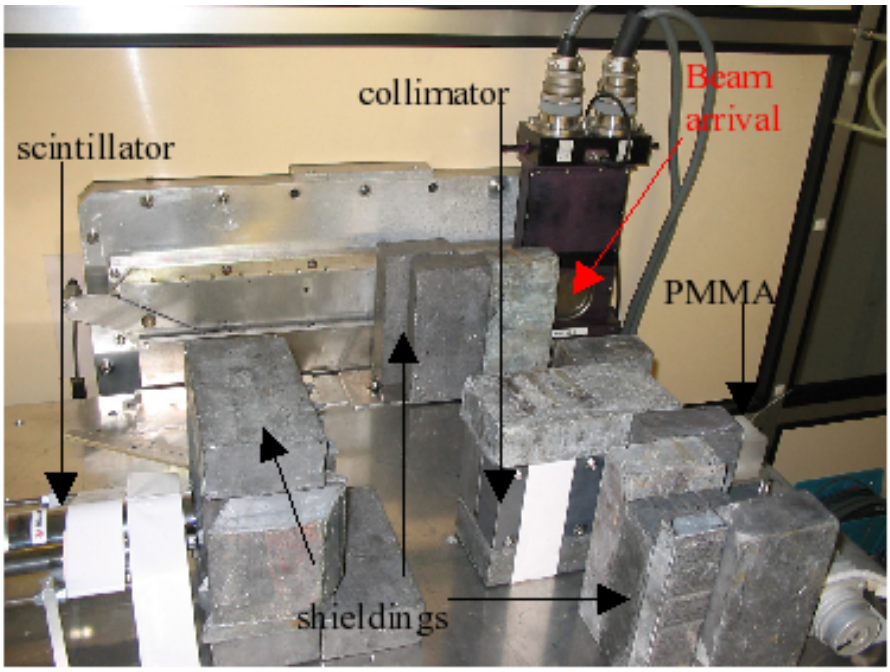

Figure 7.1: Setup used in June 2007 at GANIL

the spatial resolution of the dose fall-off is typically of 1mm and the counting rates seems high enough: improvements of the detection efficiency should lead to counting rates that allow a real-time control of hadrontherapy. The studies planned for the next experiments are the following:

- feasibility of the neutron/γ discrimination with pulse shape analysis,
- improvement of the accuracy of the counting rate measurements per solid angle unit,
- complementary information on the radiative life time of the excited fragments.

Concerning the long term developments, the choice of the detection system is still open. Two systems can be considered: the gamma camera or the multi-Compton telescope widely used in astrophysics. The group of the INSA institute is currently performing Geant4 simulations to evaluate the feasibility of the hadrontherapy control with a multi-Compton telescope and the study of dedicated image reconstruction is planned.

Chapter 8

Conclusion

So far two different approachs have been used to deal with quality control in hadrontherapy centres: in- beam dedicated PET and off-beam commercialPET. In-beam PET offers many advantages but experience at GSI and work presented in [1] shows that it demands dedicated non obvious developpements in order to cope with geometry and detector constraints, and especially to adapt the data acquisition to supress random coincidences during ions delivery.
Getting further is aiming at the real-time in-beam PET. First point to be adreesed is the statistics that one can expect. It is not yet clear if real-time can be acheived with the currently used acquisition techniques. Improvements of detectors efficiency or hermiticity could be necessary. A second point is the image reconstruction, currently the standard PET images reconstruction are far from real-time. The use of the time of flight information, available with the last generation of detectors, will allow to gain orders of magnitude in computing time. This, combinated with efforts on algorithms and code optimisation (parallelisation) and last generation computers, could help to really deliver every few seconds an image of good quality.
Other instrumentation than PET can also be envisaged, using for instance the information carried by the gamma prompt. One other source of information can be the ion beam itself, if beam instrumentation get more precise (in time, energy and localisation). These additionnal information could be either used in complementary techniques or integrated to the same image for instance in order to speed up the reconstruction process.
The real-time in-beam PET represents a real challenge in various domains. Detailed studies, with both simulations and experiments, would be needed to define precisely the necessary improvements or new developpements. At this time, we can obviously not yet conclude on the feasability of a real-tile in-beam PET for hadrontherapy quality control, it seems that possibilities are present and are worth to be explored.

Bibliography

[1] Paulo Alexandre Vieira Crespo. *Optimisation of in-beam positron emmission tomography for monitoring heavy ion tumor therapy.* PhD thesis, Technischen Universitt Darmstadt, 2005.

[2] Pawelke et al. Therapy monitoring with pet techniques. In *Heavy Charged Particles in Biology and Medicine Proceedings*, pages 97–105, Heidelberg, Germany, Sept 2007.

[3] S. Surti, S. Karp, L.M. Popescu, E. Daube-Witherspoon, and M. Werner. Investigation of time-of-flight benefit for fully 3-dpet. *IEEE Transactions on Medical Imaging*, 25(5):529–538, May 2006.

[4] M. Teshima, B. Dolgoshein, R. Mirzoyan, J. Nincovic, and E. Popova. Sipm development for astroparticle physics applications. In *30th International Cosmic Ray Conference*, 2007.

[5] J. Vavra, J. Beniteza, D.W.G.S. Leith, G. Mazaheria, B. Ratcliffa, and J. Schwieninga. A 30 ps timing resolution for single photons with multipixel burle mcp-pmt. *Nuclear Instruments and Methods in Physics Research Section A - accelerators spectrometers detectors and associated equipment*, 572 (1):459–462, Mar 2007.

[6] A.Y. Barnyakov, M.Y. Barnyakov, V.V. Barutkin, et al. Investigation and development of microchannel plate phototubes. *Nuclear Instruments and Methods in physics research section A -accelerators spectrometers detectors and associated equipment*, 572 (1):404–407, Mar 2007.

[7] P. Solevi. *Study for an in-beam PET system for the CNAO.* PhD thesis, University of Milano, 2007.

[8] P. M.Shikhaliev. A novel gamma-ray imaging concept using "edge-on" microchannel. *Nuclear Instruments and Methods in Physics Research Section A - accelerators spectrometers detectors and associated equipment*, 460 (2-3):465–468, Mar 2001.

[9] C.H. Min, C.H. Kim, M.Y. Youn, et al. Prompt gamma measurements for locating the dose falloff region in the proton therapy. *Applied Physics Letters*, 89 (18)(183517).